Effect of Nanoparticle Modification on Composite Mode II Delamination

Ying Zeng[1,2*], Hong-Yuan Liu[1], Yiu-Wing Mai[1] , Xu-Sheng Du[1]

[1]Centre for Advanced Materials Technology (CAMT), The University of Sydney, 2006, Australia
[2]Structure Department, Shanghai Aircraft Design & Research Institute, 201221, China
* Corresponding author: zengying@comac.cn

Abstract The effect of nanoparticle modification on the interlaminar shear fracture behavior of carbon fibre/ epoxy laminates were studied by the End Notched Flexure (ENF) tests. The mode II fracture toughness was improved in the presence of these nanoparticles although nano-rubber was more effective compared to nano -silica. Examination of the fracture surfaces of composite laminates by scanning electron microscopy showed no debonding of nano-silica particles but some evidence of nano-rubber cavitation. Anti-Symmetric Four-Point Bending (ASFPB) tests of the nanoparticles modified epoxies was conducted and the results indicated that nano-silica was more effective in toughening bulk epoxy, but this high toughness could not be effectively transferred to mode II delamination in the composite laminates. Finite element analysis was performed to confirm the predominant Mode II stress state of the ASFPB test.

Keywords: Mode II delamination; carbon fibre composite; silica nanoparticles; rubber nanoparticles.

1. Introduction

Fiber laminates are widely used today for their outstanding strength-to-weight ratio. However, their interlaminar weakness is a major problem limiting their service applications. Hence, many past efforts have focused on increasing the interlaminar fracture resistance. Recently, nano-sized particles are found to improve the toughness of bulk epoxies [1-4] and this has stimulated many new research activities on the potential of incorporating these nanoparticles to increase the fracture toughness of composite laminates. Thus, previous studies on mode I double-cantilever-beam (DCB) delamination tests [5-6] showed that, with nanoparticle modification of the epoxy matrix, the mode I interlaminar fracture toughness of carbon fibre composites can be improved up to 150% and 27% by rubber and silica nanoparticles, respectively [6]. But in most practical situations, delamination often happens in a mixed mode I and mode II fracture. Hence, before studying the mixed mode problem, it is important to investigate whether the nanoparticles can also increase the mode II fracture resistance.

In this paper, we present recent findings on mode II toughness of carbon fibre/epoxy laminates and corresponding bulk epoxies, which are modified by different nanoparticles: (a) nano-silica and (b) nano-rubber. End Notched Flexure (ENF) tests [7] were conducted on these composite systems and their interlaminar toughness values, G_{IIC}, were evaluated. Corresponding bulk materials without carbon fibers were investigated by the Anti-Symmetric Four-Point Bending (ASFPB) test. Finite element analysis was applied to evaluate the stress state at the crack-tip based on the ASFPB experiments. Fracture surfaces of both ENF and ASFPB samples of different material systems were studied by Scanning Electron Microscopy (SEM) to examine their toughening mechanisms and possible interactions between fibers and nanoparticles. Comparison of mode I [6] and mode II toughness was made to quantitatively study the overall delamination resistance of the fiber laminates with different matrix formulations.

2 Experimental Method

2.1 Sample preparation

The processing of the composite laminates with different matrix systems (see Table 1) for mode II testing was identical to that used in our previous work on mode I delamination [6]. The composite laminates were fabricated from plain woven carbon fibres (168058ITL supplied by Inter-Turbine Advanced Logistics Pty Ltd, Australia) with a planar density of 203 g/m^2. The epoxy resin system included Araldite-F (diglycidyl ether of bisphenol A, DGEBA) and piperidine, both supplied by Sigma-Aldrich, where the piperidine was applied as a curing agent by the weight ratio of 100:5. Two types of nanoparticles were used: 40 wt% sol-gel nano-silica (Nanopox F400, Nanoresins AG, Germany) with ~20 nm SiO_2, and nano-rubber/bisphenol A (Kaneka Corporation, Japan) with 25 wt % of ~100 nm core-shell rubber in master batches.

Eighteen-ply laminates of ~270 mm^2 were prepared by the hand lay-up method. Precautions were taken to keep the fabrics well aligned and flat. A 0.2 mm thickness Kapton® polyimide film was inserted in the mid-plane of the laminates to act as the initial crack. The laminates were wrapped with bleeders and release film within a vacuum bag, and first vacuumed in a chamber for 20 min followed by curing in a hot-press at 120 ºC for 16 h. High curing temperature excursions for long durations were applied to ensure the resin was fully cured. A pressure of 250 kPa was applied during curing to maintain a uniform laminate thickness and a constant fiber volume fraction, which were 0.19 mm and 60±1%, respectively. 120x20 mm^2 ENF samples were finally cut from the square panels by a wet diamond saw.

The bulk materials prepared for ASFPB testing were the same as the matrices of the laminates. Material formulations were prepared by mixing plain DGEBA resin with required amounts of nano-silica or nano-rubber master batch. After adding the curing agent to the blend, the mixture was poured into a preheated mould for curing at 120 °C for 16 h identical to the laminates. A pre-crack was made under the requirements of the test on the middle of each specimen with a sharp blade.

Table 1 Matrix formulation of carbon fibre laminates

Material Code	Matrix Formulation by Weight Percentage (%)		
	Epoxy	Silica	Rubber
E* (control)	100	--	--
S6	94	6	--
S8	92	8	--
S10	90	10	--
S12	88	12	--
R6	94	--	6
R8	92	--	8
R10	90	--	10
R12	88	--	12

*E represents neat epoxy resin matrix.

2.2 Fracture toughness measurements

Three-point ENF tests

Standard 3-point ENF tests were performed in an Instron 5567 machine according to the Protocol for Interlaminar Fracture Testing No. 2 (1992) [7]. Fig. 1 shows the geometry and dimensions of the ENF sample. The initial crack length a is 25 mm and a/L = 0.5. The crack mouth opening displacement rate was 0.5 mm/min. 5 samples were tested for each matrix system and their load-displacement curves were recorded. The interlaminar toughness, G_{IIC}, was calculated according to

the protocol [7] by:

$$G_{IIC} = \frac{9a^2\delta P}{2b(2L^3+3a^3)} \cdot \frac{1-0.6099\times\left(\delta/L\right)^2}{1+0.3766\times\left(\delta/L\right)^2} \quad (1)$$

where δ and P are displacement and maximum force recorded at the load-point at fracture.

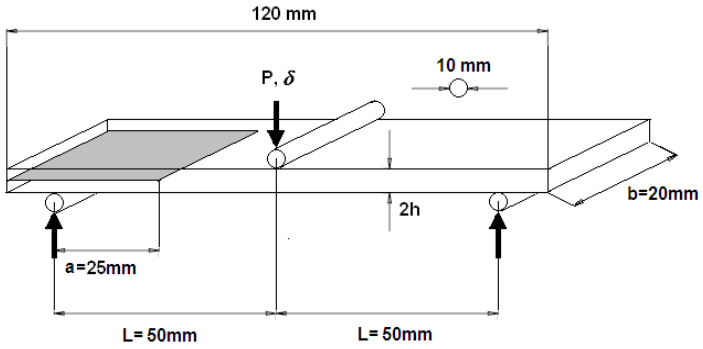

Figure 1. Dimensions of ENF specimen.

Four-point ASFPB tests

ASFPB tests were conducted on bulk materials with pre-cracked specimens, 90(L)x6(B)x16(W) mm^3, as shown in Fig. 2. The loading distance S_2/W = 0.75; S/W=3 was chosen and the pre-crack length was strictly limited to within $0.53 \le a/W \le 0.75$ based on previous studies [8-10] in order to provide a pure in-plane shear stress field around the crack-tip which would induce a high K_{II}/K_I ratio (over 20) [8]. Thus, it is reasonable to consider the ASFPB test as pure mode II fracture under such a geometric configuration since mode I fracture can be essentially neglected. Hence, according to [10], the mode II stress intensity factor can be calculated from:

$$K_{II} = F_{II}\tau_0\sqrt{\pi a} \quad (2)$$

where

$$F_{II} = -0.2915 + 6.33229\frac{a}{W} - 9.1199\left(\frac{a}{W}\right)^2 + 6.0570\left(\frac{a}{W}\right)^3$$

$$\tau_0 = \frac{P_1 - P_2}{WB} \quad P_1 = \frac{S_1}{S}P\,; \quad P_2 = \frac{S_2}{S}P$$

We assume $K_{IIC} \approx K_{II}$ when P is substituted with the maximum load at fracture. The tests were conducted on an Instron 5567 at a speed of 0.5 mm/min at the load-point.

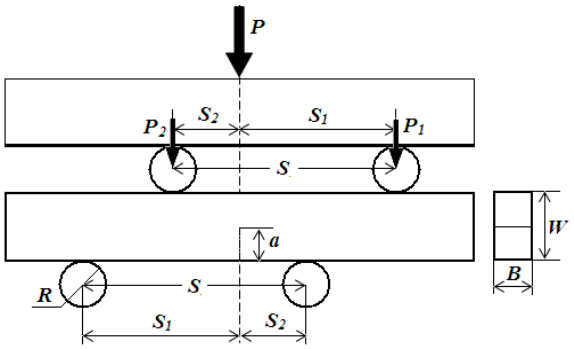

Figure 2. Dimensions of ASFPB specimen.

2.3 Finite Element Analysis (FEA)

The stress state for the mode II ASFPB test was simulated using ABAQUS. The geometry of the model is the same as the test sample, which is 90(L)x6(B)x16(W) mm^3. Since the ASFPB sample is symmetric to the central crack line, two parts were built and partially tied together to form a 10 mm crack. The loads, P_1 and P_2, were applied over contact areas, 2x6 mm^2 and 1x6 mm^2, respectively, aligned with the impressions left on the sample after the test. Young's modulus was chosen as 2.6 GPa to simulate the stress distribution, which was found insensitive to modulus verification within a small range (~10%) due to the plane strain feature of the FEA model. The average maximum load at fracture during the experiments (1200 N) was applied in the simulation study. Hence, the resultant stress distribution obtained in FEA should show the stress state at fracture initiation.

2.4 Microstructure analysis

The fracture surfaces of the fibre composites and the bulk samples were coated with a thin gold layer and examined by SEM (Zeiss ULTRA Plus SEM) at an accelerated voltage of 2 kV.

3 Results and Discussion

3.1 Carbon fiber laminates

Load-displacement curves of the ENF tests were recorded with an Instron 5567. The maximum load P and corresponding displacement δ from each load-displacement curve were substituted into Eq. (1) with the initial crack length a to obtain G_{IIC} for each specimen. According to the protocol [7], the crack length a is measured after the test by opening the sample. The average value of 4 samples was reported as the mode II fracture toughness of the corresponding material system.
In Fig. 3, calculated G_{IIC} values with standard deviations of nano-silica and nano-rubber modified fiber laminates are compared with their G_{IC} values [6]. In mode II fracture, the silica nano-particles are not as effective as they are in mode I, Fig. 3(a). G_{IIC} increases with increasing nano-silica loading until it reaches a maximum at 10 wt% silica, which is ~8% higher than the control. Further increase of silica loading lowers G_{IIC}. This trend is similar to the mode I results [6]. Mode II fracture toughness of nano-rubber modified fiber laminates are shown in Fig. 3 (b). Unlike silica, nano-rubber particles can improve G_{IIC} by as much as 43% higher than the control at 8 wt%. Again, higher nano-rubber loading cannot improve G_{IIC}; and at 12 wt%, G_{IIC} is even lower than the control. These results should be viewed with caution since at 12 wt% of nano-rubber or nano-silica uniform dispersion of these particles was difficult to achieve, which would lead to reduced toughness values. It is further noted that with pure epoxy matrix, G_{IC} of the composite laminates is ~54% lower than G_{IIC}. For silica modified epoxy matrix, the mode I delamination resistance G_{IC} is ~48-50% of the mode II delamination, G_{IIC}. However, the differences between G_{IC} and G_{IIC} of nano-rubber filled composites, R6, R10 and R12, are less than 10%. Indeed, G_{IC} of R12 is even slightly higher than G_{IIC}. Hence, nano-rubber modified composite laminates can provide superior mode I and mode II toughness, e.g., R8 and R10, which is not possible in nano-silica laminates.

3.2 Bulk materials

The mode II fracture toughness, G_{IIC}, of the bulk materials, which are the same as the matrix of the composites, was determined by the ASFPB tests. The results are listed in Table 2 with ±1standard deviation, where the K_{IIC} values were calculated using Eq. (2). To compare to the toughness of the corresponding fiber composites, the critical stress intensity factors K_{IIC} of bulk materials are converted to the fracture energy G_{IIC} (see Table 2) by:

$$G_{IIC} = \frac{(1-\mu^2)K_{IIC}^2}{E} \tag{3}$$

where μ is Poisson's ratio and E is Young's modulus. In the calculations, the values of Poisson's ratio of different material systems were obtained by the simple rule of mixture based on the density, Poisson's ratio and volume percentage of the epoxy and particles [4]. Note that the ratio of K_I/K_{II} at fracture is less than 4%, indicating that the ASFPS geometry is suitable for mode II toughness evaluation.

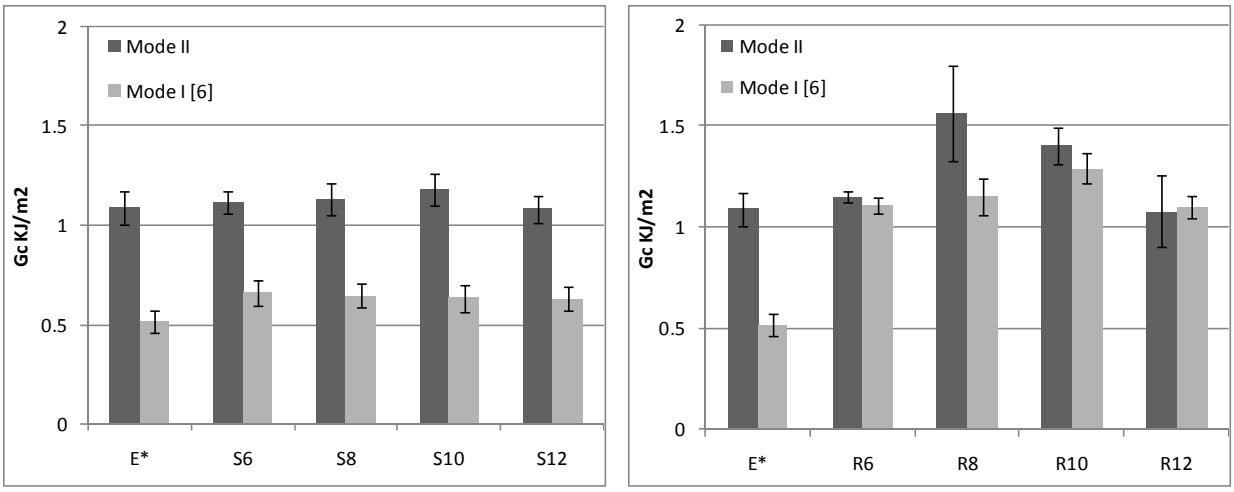

(a) Nano-silica modified system (b)Nano-rubber modified system

Figure 3 Comparisons between G_{IIC} and G_{IC} [taken from [6]] of nanoparticles modified composites.

Table 2. Mode II fracture toughness of the bulk material.

Material Code	K_{IIC} (MPa $\sqrt{m}$)	K_I/K_{II}	E (GPa) [4]	G_{IIC} (kJ/m^2)
E*	3.53 (±0.23)	0.031	2.86	3.82
S10	4.18 (±0.21)	0.044	3.14	4.88
R10	2.78 (±0.21)	0.035	2.30	2.95

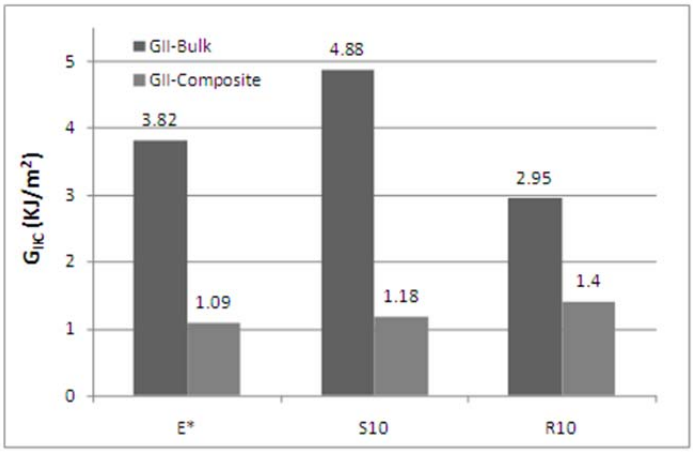

Figure 4. Comparison of G_{IIC} of bulk and composite laminates.

Figure 4 compares the mode II fracture toughness G_{IIC} of the bulk materials (neat epoxy and nanoparticle modified epoxy) and their fibre composite laminates. Notably, the fracture energy is improved by nano-silica modification in S10 as bulk; however, G_{IIC} of the S10 composite laminate is 76% less than that of the corresponding bulk materials. Thus, the toughness transfer efficiency in mode II of S10 is much lower than that in mode I [6], where the G_{IC} of fibre composite is more than 94% of the corresponding bulk. The nano-rubber filled epoxy has a higher transfer efficiency of ~50% from bulk to composite laminate, but the incorporation of rubber particles decreases the bulk G_{IIC} when compared to pure epoxy.

FEA was applied to understand the stress state of mode II ASFPB test. Figures 5(a)-(c) show the distributions of normal stresses, σ_x and σ_y, and shear stress, τ_{xy}, respectively. The crack tip stresses have been discussed in [11]. At fracture initiation, the crack-tip is subjected to a local tensile stress σ_x of ~5 MPa, (see Figure 5(a)), but the shear stress τ_{xy} is most dominant, which is ~30 MPa. The FEA results confirm that the samples failed primarily due to mode II fracture.

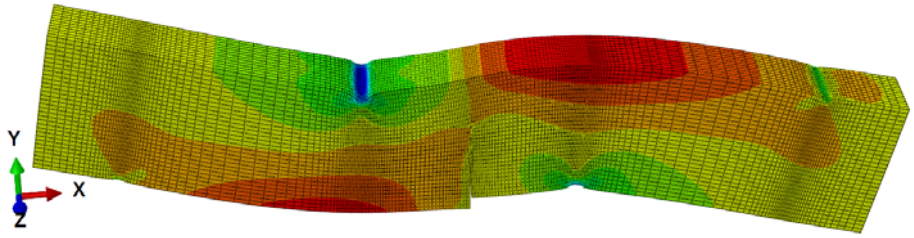

(a) Distribution of normal stress σ_x.

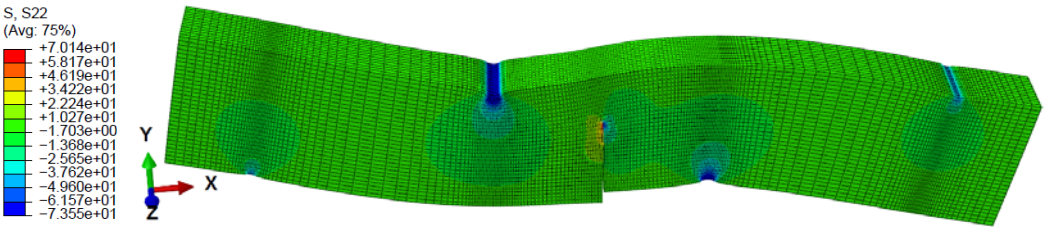

(b) Distribution of normal stress σ_y.

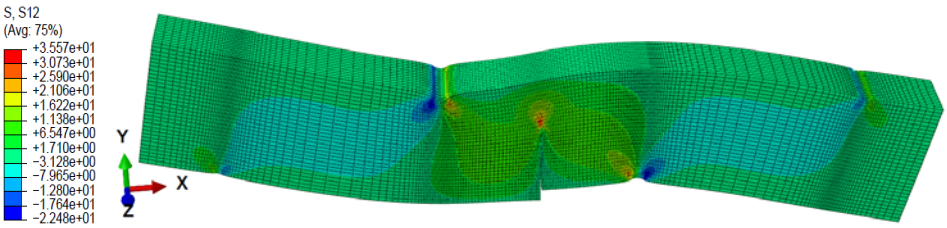

(c) Distribution of shear stress τ_{xy}

Figure 5 General stress distribution of mode II ASFPB specimen.

3.3 Fractograph study

Two matrix formulations were chosen to study the effects of nanoparticles on ENF tests: 10 wt% silica (S10) and 10 wt% rubber in epoxy (R10), in comparison with the control laminate (E*). In mode II fracture, there is good bonding observed between fiber and matrix for all composites and no separations can be seen in Figs. 6(a)-(c). However, obvious debonding between fibers and rubber modified matrix was observed in our previous study on mode I delamination [6] possibly due to the different fracture mode. Since the cracks are not open in mode II, fiber pullout from the matrix is difficult. Fig. 6(a) shows the fracture surface of the composite laminates, where silica nanoparticles

are evenly dispersed in the matrix. No particle debonding or pullout can be found in Fig. 6(a), where the nano-silica particles are well covered by epoxy. Since silica nanoparticle debonding is the major toughening mechanism in mode I [4-6], Fig. 6(a) therefore explains why the improvement of fracture toughness of these composites in mode II is not as remarkable when compared to the laminates with unmodified epoxy matrix. In contrast, nano-rubber particles in mode II fracture surface are observed to be well-dispersed in epoxy in Fig. 6(b). However, it is difficult to ascertain if the nano-rubber particles are cavitated, though some evidence exists when examined on much higher magnification. Another possible reason for the increase in toughness of R10 is the micro-voids introduced during processing of the laminates. When the rubber particles were added to epoxy, the viscosity of the resin was increased which made the resin flow between the fibres more difficult. More air bubbles and voids might form in the laminates. During delamination propagation, these voids may reduce the stress intensity at the crack tip and delay the delamination growth. However, further examination on the composite microstructure before and after testing are needed to prove the above hypothesis.

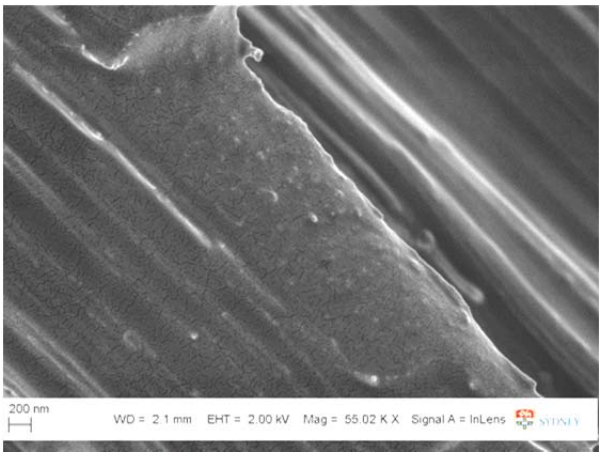

(a) Fracture surface of carbon fiber/S10 composite.

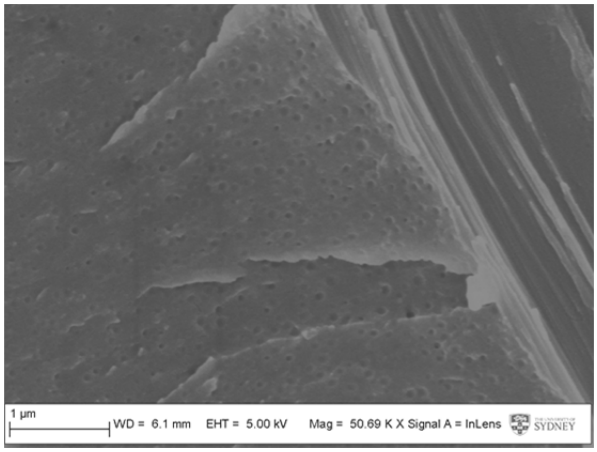

(b) Fracture surface of carbon fibre/R10 composite.

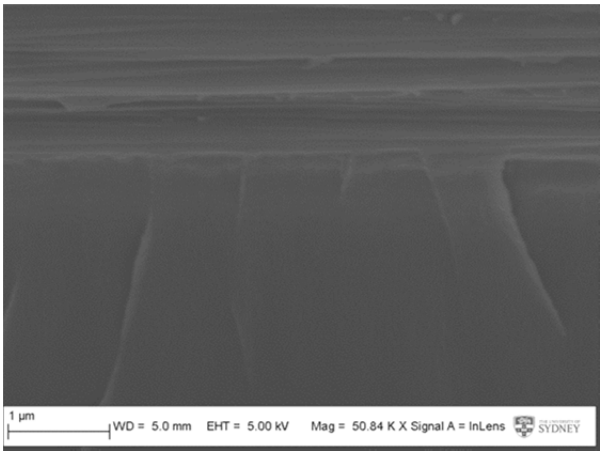

(c) Fracture surface of carbon fibre/E* composite.

Figure 6. Fractographs of ENF mode II specimens.

Figs. 7(a)-(c) show fracture surfaces of mode II ASFPB specimens of pure epoxy (E*), nano-rubber and nano-silica modified epoxies (R10 and S10) by optical microscopy under low magnification (x6) on the left side and high magnification (x750) by SEM on the right side. Pure epoxy shows typical brittle fracture characteristics in Fig. 7(a). Silica modified bulk epoxy shows the roughest surface; however, no typical silica debonding is observed in Fig. 7(b) even at higher resolution. In Fig. 7(c),

the rubber modified sample shows clear stress-whitened area in the center of the crack tip, indicating plastic deformation occurred during mode II fracture. R10 also possesses the smoothest near crack-tip region, which agrees with the test results where rubber modified epoxy shows the lowest G_{IIC}.

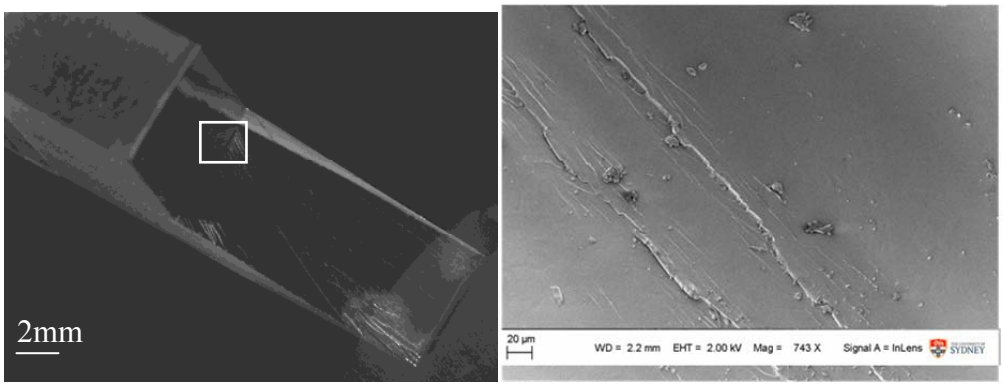

(a) Crack tip of E*.

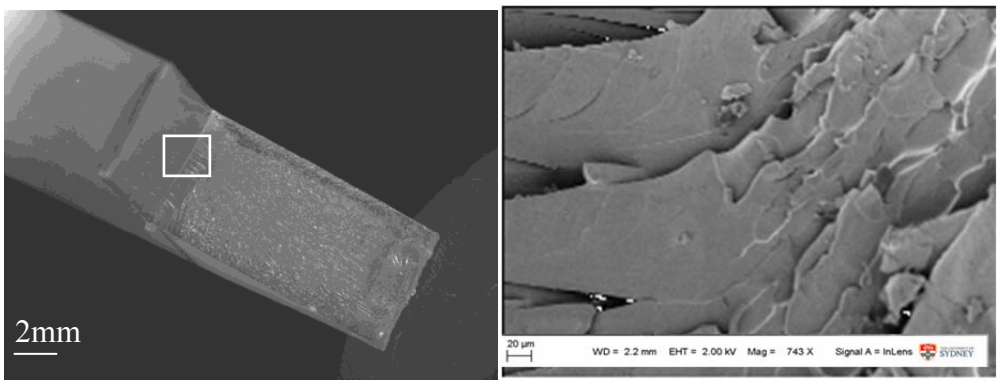

(b) Crack tip of S10.

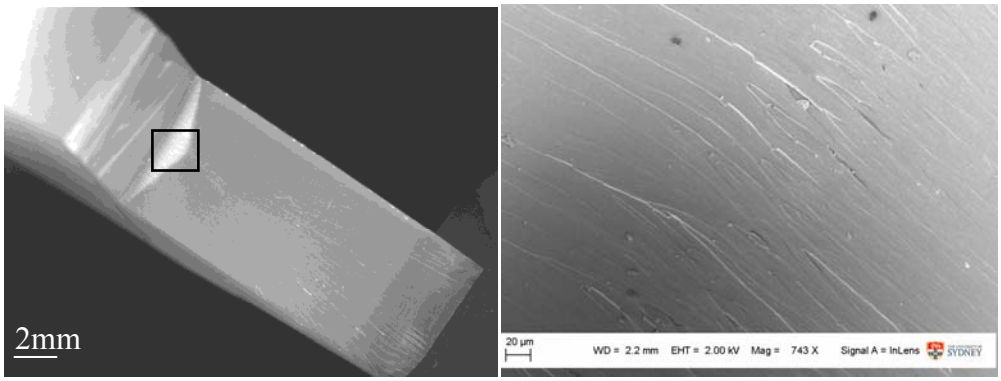

(c) Crack tip of R10.

Figure 7. Crack tip of bulk ASFPB specimens.

4 Conclusion

Mode II fracture behaviors of nanoparticles modified carbon fibre laminates have been studied by the ENF tests. Additional mode II ASFPB tests were also conducted on the nanoparticles modified bulk epoxies. From the results obtained we can conclude below:

(a) Nano-rubber modified epoxy is effective in enhancing the mode II toughness, G_{IIC}, of composite laminates depending on the particle loading. For example, R8 increases G_{IIC} by over 40% compared

to E*. By contrast, nano-silica modified epoxies are not as effective and only less than 8% improvement on G_{IIC} can be achieved.
(b) Mode II toughness G_{IIC} of nano-silica modified epoxy composite laminates are approximately twice the mode I toughness G_{IC} independent of the particle loading. The ratio of G_{IIC}/G_{IC} for nano-rubber modified epoxy composite laminates is much less.
(c) Nano-silica particles increase significantly G_{IIC} of the bulk epoxy; but this high toughness cannot be effectively transferred to the delamination toughness of the nano-silica modified epoxy composite laminates.
(d) Regarding the toughening mechanisms, silica particle debonding and rubber cavitation are not clearly shown by the SEM photos of mode II fracture surfaces, although thyeare the major toughening mechanisms in Mode I fracture of nanoparticle modified epoxy [6] and their fibre composites [4]. Further study will be conducted to identify the main reasons for the increase of G_{IIC} in S10 (bulk) and R10 (composites laminates).

Acknowledgements

Y Zeng would like to thank colleagues at the University of Sydney and the Shanghai Aircraft Design & Research Institute for their support and helpful discussions. H-Y Liu wishes to thank the Australian Research Council (ARC) for the support of this project through a Future Fellowship awarded to her (FT0992081, 2009-2013) tenable at the University of Sydney. Finally, the authors wish to acknowledge Nanoresin AG, Germany for the supply of nanosilica particles for this study.

References

[1] H. Zhang, L-C. Tang, Z. Zhang, K. Friedrich and S. Sprenger, Fracture behaviours of in situ silica nanoparticle-filled epoxy at different temperatures, Polymer, 2008, 49, 3816-3825.
[2] Y.L. Liang and R.A. Pearson, Toughening mechanisms in epoxy-silica nanocomposites (ESNs), Polymer, 2009, 50, 4895-4905.
[3] J-L. Tsai, H. Hsiao and Y-L. Cheng, Investigating mechanical behaviours of silica nanoparticle reinforced composites, Journal of Composite Materials, 2010, 44 (4), 505-524.
[4] H-Y. Liu, G-T. Wang, Y-W. Mai, Y. Zeng, On fracture toughness of nano-particle modified epoxy. Composites Part B: Engineering. 2011;42(8):2170-5.
[5] T.H. Hsieh, A.J Kinloch, K. Masania, J.S. Lee, A.C. Taylor and S. Sprenger, The toughness of epoxy polymers and fibre composites modified with rubber microparticles and silica nanoparticles, Journal of Material Science, 2010, 45, 1193-1210.
[6] Y. Zeng, H-Y. Liu, Y-W. Mai, X-S. Du. Improving interlaminar fracture toughness of carbon fibre/epoxy laminates by incorporation of nano-particles. Composites Part B: Engineering. 2012;43(1):90-4.
[7] Protocol for interlaminar fracture testing No.2, Mode II (ENF), 1992.
[8] M.R. Ayatollahi, S. Shadlou, M.M. Shokrieh. Fracture toughness of epoxy/multi-walled carbon nanotube nano-composites under bending and shear loading conditions. Materials & Design. 2011;32(4):2115-24.
[9] W. Araki, D. Asahi, T. Adachi, A. Yamaji. Time-temperature dependency of mode II fracture toughness for bisphenol A type epoxy resin. Journal of Applied Polymer Science. 2005;96(1):51-5.
[10] Y. Murakami, E.d. Pergamon. Stress Intensity Factors Handbook; Oxford, England, 1987; p 941
[11] H.S. Kim, P. Ma. Mode I and II fracture behaviour of rubber modified brittle epoxies. In: Ye L, Mai Y-W, editors. Polymer Blends and Polymer Composites1998. p. 179-86.